Bioconjugate Chemistry

Article

pubs.acs.org/bc

Enzyme-Mediated Methodology for the Site-Specific Radiolabeling of Antibodies Based on Catalyst-Free Click Chemistry

Brian M. Zeglis,[†] Charles B. Davis,[†] Robert Aggeler,[‡] Hee Chol Kang,[‡] Aimei Chen,[‡] Brian J. Agnew,[‡] and Jason S. Lewis*[,†]

[†]Department of Radiology and the Program in Molecular Pharmacology and Chemistry, Memorial Sloan-Kettering Cancer Center, New York, New York, United States

[‡]Foundational Biology Group, Molecular Probes-Life Technologies, Eugene, Oregon, United States

Supporting Information

ABSTRACT: An enzyme- and click chemistry-mediated methodology for the site-selective radiolabeling of antibodies on the heavy chain glycans has been developed and validated. To this end, a model system based on the prostate specific membrane antigen-targeting antibody J591, the positron-emitting radiometal ^{89}Zr, and the chelator desferrioxamine has been employed. The methodology consists of four steps: (1) the removal of sugars on the heavy chain region of the antibody to expose terminal *N*-acetylglucosamine residues; (2) the incorporation of azide-modified *N*-acetylgalactosamine monosaccharides into the glycans of the antibody; (3) the catalyst-free click conjugation of desferrioxamine-modified dibenzocyclooctynes to the azide-bearing sugars; and (4) the radiolabeling of the chelator-modified antibody with ^{89}Zr. The site-selective labeling methodology has proven facile, reproducible, and robust, producing ^{89}Zr-labeled radioimmunoconjguates that display high stability and immunoreactivity *in vitro* (>95%) in addition to highly selective tumor uptake (67.5 ± 5.0%ID/g) and tumor-to-background contrast in athymic nude mice bearing PSMA-expressing subcutaneous LNCaP xenografts. Ultimately, this strategy could play a critical role in the development of novel well-defined and highly immunoreactive radioimmunoconjugates for both the laboratory and clinic.

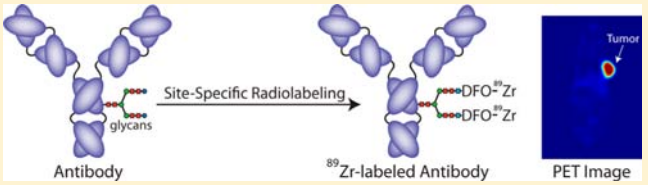

INTRODUCTION

The remarkable selectivity, affinity, and stability of antibodies have made them extremely promising vectors for the delivery of diagnostic and therapeutic radioisotopes to tumors.[1] Indeed, over the past two decades, antibodies bearing radionuclides ranging from ^{124}I, ^{111}In, and ^{64}Cu for PET and SPECT imaging to ^{90}Y, ^{177}Lu, and ^{225}Ac for radiotherapy have been successfully developed and translated to the clinic.[2]

One important limitation to the development and translation of radioimmunoconjugates, however, is the lack of site-selectivity in the radiolabeling of antibodies. The vast majority of antibody radiolabeling methods rely on reactions with amino acids, typically tyrosines for radioiodinations or lysines for radiometal chelator conjugations. Yet antibodies are, of course, very large molecules and thus possess multiple copies of each of these amino acid residues.[3] Consequently, precise control over the exact molecular location of the radionuclides or radiometal-chelator complexes on the antibody is impossible. This lack of site-selectivity presents two principal complications to the development, validation, and clinical utilization of radioimmunoconjugates. First, without the ability to control the precise location of the radiolabel on the antibody, radioisotopes or radiometal chelates may become appended to the antigen-binding region of the antibody, adversely affecting the immunoreactivity of the construct. Second, without knowledge of the exact site of radiolabeling, the resultant radioimmunoconjugates remain somewhat inadequately chemically defined, which can pose a problem during basic scientific investigations and the preclinical development of radioimmunoconjugates. In addition, while a number of non-site-specifically radiolabeled immunoconjugates are currently in use in the clinic, it is very likely that the development of site-specifically labeled conjugates that are well characterized and precisely chemically defined will prove valuable in the regulatory review and approval process.

Further, the lack of reproducibility offered by either direct labeling reactions or chelator conjugation strategies presents another troubling limitation to current strategies for the construction of radioimmunoconjugates. Given the non-site-selective nature of most radiolabeling methodologies, each new immunoconjugate must undergo extensive optimization in order to obtain a degree of labeling that strikes a suitable balance between the specific activity of the final radioimmunoconjugate and its immunoreactivity, a process which can be time-consuming, tedious, and costly. Further, labeling reagents themselves tend to be chemically unstable and subject to hydrolysis, thus requiring storage under inert atmospheres of argon or nitrogen.

In response to these issues, extensive efforts have been made to develop robust and reliable site-selective radiolabeling

Received: March 6, 2013
Revised: April 26, 2013
Published: May 17, 2013

dx.doi.org/10.1021/bc400122c | *Bioconjugate Chem.* 2013, 24, 1057−1067

methodologies for antibodies.[4−10] With few exceptions, these strategies rely on antibodies that have been specially engineered to bear either reactive thiol moieties or fusion proteins. These systems are creative and have proven successful; however, the use of genetically engineered antibodies adds undue layers of complexity and expense that hamper both the modularity and potential for clinical translation of the systems. To circumvent these issues, we have chosen to focus on a handle for site-specific antibody modification that has remained somewhat, though not completely, neglected in the development of radiolabeling strategies: the heavy chain glycans.

Immunoglobulin G antibodies (IgGs) contain a conserved *N*-linked glycosylation site on the CH2 domain of each heavy chain of the Fc region. *N*-linked oligosaccharides from a variety of different animal species show a heterogeneous mixture of biantennary complex-type oligosaccharides.[11] In general, the number of sialylated oligosaccharides is significantly lower compared to the number of neutral sugar species, and high-mannose type oligosaccharides are absent (except in chickens).[11] Although heterogeneous with respect to their core fucose, sialic acid, and galactose monomers, the majority of these biantennary glycans are composed of the G0, G1, or G2 isoforms (i.e., 0, 1, or 2 terminal galactose residues, respectively), with the specific ratio of isoforms dependent on species and physiological status.[11] Since IgG glycans are located on the heavy chain Fc domain of the antibody—far from the antigen binding domains—they provide extremely attractive targets for site-selective chemical modification, and indeed, a number of conjugation methodologies have been developed to exploit this.[12] For example, one fairly commonly used modification strategy is predicated on the oxidation of vicinal alcohols on the sugar chains to aldehydes, followed by subsequent labeling via reductive amination or hydrazide condensation reactions. This methodology, however, requires prolonged exposure of the antibody to low pH and harsh redox conditions (e.g., treatment with periodate and cyanoborohydride) and can result in nonselective modifications to amino acid side chains in the antibody. These, of course, are seriously limiting factors, as the former can adversely affect the immunoreactivity of the antibody, and the latter can defeat the purpose of the site-selective modification strategy entirely.[13]

An alternative procedure for the site-selective modification of the IgG heavy chain glycans can be envisioned using a system based on unnatural UDP-sugar substrates and a substrate-permissive mutant of β-1,4-galactosyltransferase, GalT(Y289L), first designed, engineered, and expressed by Ramakrishnan and Qasba.[14] This glycoengineering strategy has been used by a variety of researchers in a number of different settings, including the detection of post-translational modifications, the site-specific bioconjugation of immunoglobulins, the rapid identification of *O*-GlcNAc-glycosylated proteins in cell lysates, and the exploration of glycosylation patterns in the brain.[15−24] In 2003, for example, Hsieh-Wilson and co-workers employed this system to selectively biotinylate proteins with post-translational *O*-GlcNAc modifications and then identify them using a horseradish peroxidase-based chemiluminescence reporter system.[18] In more recent work, Qasba and co-workers have employed the substrate permissive GalT(Y289L) enzyme along with a C2-keto-galactose sugar in order to site-specifically modify both full IgGs and single chain antibodies with biotinylated and fluorescent reporter moieties.[16,17,23,25]

Perhaps not surprisingly, the intersection of this glycoengineering technology and bioorthogonal click chemistry has already proven fertile ground.[15,26,27] In 2008, for example, Clark et al. used the azide-bearing UDP-*N*-acetylgalactosamine analog UDP-GalNAz (Scheme 1A) and an alkyne-modified

Scheme 1. (A) Structures of UDP-GalNAz and DIBO-DFO. (B) Strain-Promoted, Catalyst-Free Click Ligation Between UDP-GalNAz and DIBO-DFO[a]

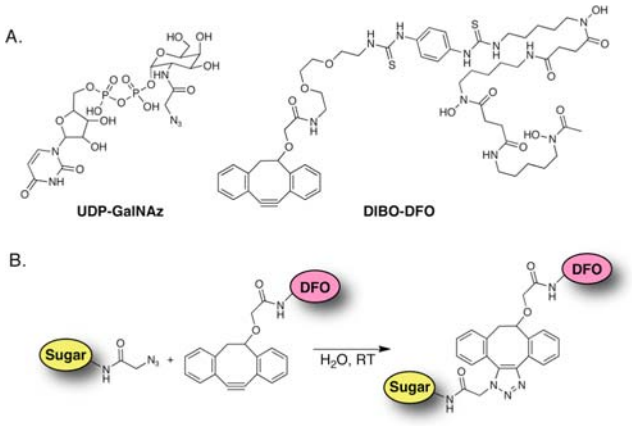

[a]DIBO = dibenzocyclooctyne; UDP = uridine-5′-diphosphate; GalNAz = *N*-azidozacetylgalactosamine; DFO = desferrioxamine.

fluorescent reporter to create a system for the detection, proteomic analysis, and cellular imaging of *O*-GlcNAc-modified proteins using canonical Cu-catalyzed azide−alkyne [3 + 2] cycloaddition click chemistry.[15] Importantly, however, while the copper-catalyzed azide−alkyne click reaction has been shown to be selective and efficient, it is well-known that the presence of both copper(I) and copper(II) can damage proteins and thus interfere with the structure and function of enzymes, fluorescent proteins, and antibodies. Furthermore, and more specific to radiochemical applications, the Cu-catalyzed variant of this click reaction cannot be used in conjunction with radiometal chelators, as the presence of micromolar levels of Cu catalyst can interfere with the chelation chemistry of radiometals that are often present in extremely low concentrations.[28] In recent years, the limitations of the Cu-catalyzed Huisgen cycloaddition reaction have been circumvented through the work of Bertozzi and Boons on the strain-promoted azide−alkyne click reaction: a selective, bioorthogonal, and catalyst-free ligation between an azide and a strained cyclic alkyne such as dibenzocyclooctyne.[29−31] Interestingly, a large volume of work exists on the strain-promoted azide−alkyne reaction between cyclic alkynes and GalNAz-modified biomolecules. However, in these cases, GalNAz is not employed as a substrate for GalT(Y289L); rather, these applications exploit the promiscuity of the hexosamine biosynthetic pathway to metabolically tag *O*-GlcNAc-modified proteins with azides for subsequent labeling *in vitro* or *in vivo*.[20,29,31−33]

Herein, we present a methodology for the site-selective radiolabeling of antibodies utilizing a method that combines both enzyme-mediated GalNAz incorporation and bioorthogonal, strain-promoted, copper-free azide/alkyne cycloaddition click chemistry. The procedure consists of four simple steps: (1) the enzymatic removal of terminal galactose residues on the Fc domain to expose terminal GlcNAc residues; (2) the enzymatic incorporation of GalNAz monosaccharides onto the terminal GlcNAc residues; (3) the catalyst-free, strain-promoted click conjugation of novel chelator-modified

dibenzocyclooctynes (DIBO) to the GalNAz residues; and (4) the radiolabeling of the chelator-modified construct with an appropriate radiometal (Schemes 1 and 2). Because all

Scheme 2. Four Step Strategy for the Site-Selective, Enzyme- and Click Chemistry-Mediated Radiolabeling of Antibodies on the Heavy Chain Glycans

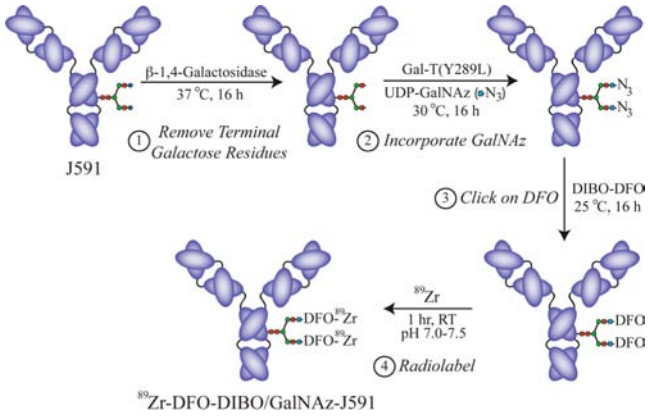

antibodies possess *N*-linked glycans located only on the heavy chain Fc region, this methodology is site-selective and critically, unlike previous systems, requires no special antibody engineering. Further, we demonstrate here that this labeling method is mild, facile, and highly reproducible, and the sites of labeling are easily and rapidly characterized. Taken together, we believe that this modular and robust labeling methodology could play a critical role in the development of novel radioimmunoconjugates and at the same time provide considerable time and cost savings by eliminating cumbersome optimization and characterization steps.

EXPERIMENTAL PROCEDURES

Reagents and General Procedures. All chemicals, unless otherwise noted, were acquired from Sigma-Aldrich (St. Louis, MO) and were used as received without further purification. All water employed was ultrapure (>18.2 MΩ cm^{-1} at 25 °C), all DMSO was of molecular biology grade (>99.9%), and all other solvents were of the highest grade commercially available. Deimmunized J591 was obtained through MSKCC's Clinical Research Department/Weill Cornell Medical College. All other antibody samples were obtained from Life Technologies, Inc. (Eugene, OR) and used as received. DIBO-NH_2 (Click-IT Amine DIBO Alkyne) was obtained from Life Technologies (Eugene, OR), and *p*-SCN-DFO was obtained from Macrocyclics, Inc. (Dallas, TX). The plasmid for GalT(Y289L) was obtained from Dr. P. K. Qasba, and the protein was obtained from Life Technologies, Inc., where it was expressed and purified according to published protocols.[34] Click-IT Alexa Fluor-488 DIBO-Alkyne was obtained from Life Technologies, Inc. (Eugene, OR). All instruments were calibrated and maintained in accordance with standard quality-control procedures. UV−vis measurements were taken on a Thermo Scientific NanoDrop 2000 Spectrophotometer. High resolution mass spectrometry measurements were performed on a Waters SYNAPT High Definition MS System (ESI-QTOF).

^{89}Zr was produced at Memorial Sloan-Kettering Cancer Center on an EBCO TR19/9 variable-beam energy cyclotron (Ebco Industries Inc., British Columbia, Canada) via the ^{89}Y(*p*,*n*)^{89}Zr reaction and purified in accordance with previously reported methods to yield ^{89}Zr with a specific activity of 5.3−13.4 mCi/μg (195−497 MBq/μg).[35] Activity measurements were made using a Capintec CRC-15R Dose Calibrator (Capintec, Ramsey, NJ). For accurate quantification of activities, experimental samples were counted for 1 min on a calibrated Perkin-Elmer (Waltham, MA) Automatic Wizard^2 Gamma Counter. Labeling of antibodies with ^{89}Zr was monitored using silica-gel impregnated glass-fiber instant thin-layer chromatography paper (Pall Corp., East Hills, NY) and analyzed on a Bioscan AR-2000 radio-TLC plate reader using Winscan Radio-TLC software (Bioscan Inc., Washington, DC). All experiments performed on laboratory animals were performed according to a protocol approved by the Memorial Sloan-Kettering Institutional Animal Care and Use Committee (protocol 08−07−013).

Cell Culture. Human prostate cancer cell line LNCaP was obtained from the American Tissue Culture Collection (ATCC, Manassas, VA, USA) and maintained by weekly serial passage in a 5% CO_2 (g) atmosphere at 37 °C. LNCaP cells were grown in RPMI 1640 medium supplemented with 10% fetal calf serum, 2 mM L-glutamine, 1 mM sodium pyruvate, 4.5 g/L glucose, 1.5 g/L sodium bicarbonate, and 100 U/mL of penicillin and streptomycin. Cells were harvested using a formulation of 0.25% trypsin and 0.53 mM EDTA in Hank's buffered salt solution without calcium or magnesium.

Xenograft Models. All experiments were performed under an Institutional Animal Care and Use Committee approved protocol, and the experiments followed institutional guidelines for the proper and humane use of animals in research. Six- to eight-week-old athymic nude male (Hsd: Athymic Nude-nu) mice were obtained from Harlan Laboratories (Indianapolis, IN). Animals were housed in ventilated cages, were given food and water *ad libitum*, and were allowed to acclimatize for approximately 1 week prior to inoculation. LNCaP tumors were induced on the right shoulder by a subcutaneous injection of 5.0×10^6 cells in a 200 μL cell suspension of a 1:1 mixture of fresh media:BD Matrigel (BD Biosciences, Bedford, MA). The xenografts reached ideal size for imaging and biodistribution (∼100−150 mm^3) in approximately 4 weeks.

Synthesis of DIBO−DFO. To a suspension of 1-(4-isothiocyanatophenyl)-3-[6,17-dihydroxy-7,10,18,21-tetraoxo-27-(*N*-acetylhydroxylamino)-6,11,17,22-tetrazaheptaeicosine]-thiourea (*p*-SCN-Bn-desferrioxamine, 22 mg, 27 μmol) and *N*-[2-[2-(2-aminoethoxy)ethoxy]ethyl]-2-[((11,12-didehydro-5,6-dihydrodibenzo[*a*,*e*]cycloocten-5-yl)oxy]acetamide (DIBO-NH_2, 20 mg, 54 μmol) in 1.5 mL of anhydrous DMF was added triethylamine (75 μL, 0.54 mmol), and the mixture was stirred at room temperature for 48 h. The resulting reaction mixture, which became a homogeneous solution, was added into 25 mL of ethyl acetate slowly over a 2 min period while stirring vigorously at room temperature. The resulting precipitate was collected by filtration to give the desired product (DIBO−DFO, 24 mg, 80% yield) as an off-white solid. TLC (silica gel, 15% H_2O in CH_3CN): R_f = 0.59. ^{1}H NMR (400 MHz, d_6-DMSO): δ 1.29−1.12 (m, CH2, 8H), 1.43−1.32 (m, CH2, 4H), 1.58−1.44 (m, CH2, 8H), 1.96 (s, CH3, 3H), 2.32−2.20 (m, CH2, 4H), 2.67−2.53 (m, CH2, 4H), 3.77−2.67 (m, CH2, 22H), 3.93 (d, OCHH-C(=O)), 4.05 (d, OCHH-C(=O)), 4.16−4.20 (m, CH, 1H), 7.48−7.27 (m, ArH, 10H), 7.60 (d, ArH, 1H), 7.70 (d, ArH, 1H), 7.85−7.79 (m, NH, 2H), 9.60−9.35 (m, NH, 2H), 9.70−9.60 (m, N−OH, 3H). HRMS (ESI) calculated mass for $C_{57}H_{80}N_{10}O_{12}S_2^+$ ($M+H^+$): 1161.4543: found mass: 1161.4911.

dx.doi.org/10.1021/bc400122c | *Bioconjugate Chem.* 2013, 24, 1057−1067

Synthesis of *N*-Azidoacetylgalactosamine (UDP-GalNAz). UDP-GalNAz was synthesized in accordance with previously reported methods.[32,36]

Site-Specific Antibody Modification with DFO−DIBO/GalNAz. *Glycans Modification.* J591 (1 mg, 8 mg/mL, in phosphate buffer saline [PBS], pH 7.4) was buffer exchanged into pretreatment buffer (50 mM Na-phosphate, pH 6.0) using a microspin column prepared with P30 resin (Bio-Rad 732−6008, 1.5 mL bed volume). The column was first equilibrated with 50 mM Na-phosphate, pH 6.0 and centrifuged for 3 min at 850*g*. 125 μL J591 antibody was then added and centrifuged for 5 min at 850*g*. The resultant antibody solution was supplemented with 40 μL of β-1.4-galactosidase (from *S. pneumonia* [2 mU/μL], obtained from Life Technologies, Inc., Eugene, OR) and placed in an incubator at 37 °C overnight.

GalNAz Labeling. A buffer exchange of the sample into TBS reaction buffer (20 mM Tris HCl, 0.9% NaCl, pH 7.4) was performed using a microspin column prepared with P30 resin. After the buffer exchange, the antibody (600 μg in 300 μL TBS buffer) was combined with UDP-GalNAz (40 μL of a 40 mM solution in H_2O), $MnCl_2$ (150 μL of a 0.1 M solution), and Gal-T(Y289L) (1000 μL of 0.29 mg/mL in 50 mM Tris, 5 mM EDTA (pH 8)). The final solution contained concentrations of 0.4 mg/mL antibody, 10 mM $MnCl_2$, 1 mM UDP-GalNAz, and 0.2 mg/mL Gal-T(Y289L) and was incubated overnight at 30 °C.

DIBO−DFO Ligation. The solution from the GalNAz labeling step was purified using six microspin columns prepared with P30 resin and TBS buffer (each microspin column received 250 μL of the GalNAz labeling solution). After centrifugation, the filtrates were combined to yield 1500 μL of antibody solution. Subsequently, 200 μL of DIBO−DFO solution (1.74 mg in 750 μL DMSO, 2 mM stock) was added to the combined filtrates, and this tube was incubated at 25 °C overnight.

Purification. After DIBO−DFO labeling, the completed antibody was purified via size exclusion chromatography (Sephadex G-25 M, PD-10 column, GE Healthcare) and concentrated using centrifugal filter units with a 50 000 molecular weight cutoff (Amicon Ultra 4 Centrifugal Filtration Units, Millipore Corp., Billerica, MA) and phosphate buffered saline (PBS, pH 7.4).

Nonspecific Antibody Modification with DFO-NCS. J591 (2−3 mg) was dissolved in 1 mL of phosphate buffered saline (pH 7.4), and the pH of the solution was adjusted to 8.8−9.0 with $NaHCO_3$ (0.1 M). To this solution was added an appropriate volume of DFO-NCS in DMSO (5−10 mg/mL) to yield a chelator:mAb reaction stoichiometry of 6:1. The resultant solution was incubated with gentle shaking for 30 min at 37 °C. After 30 min, the modified antibody was purified using centrifugal filter units with a 50 000 molecular weight cut off (Amicon Ultra 4 Centrifugal Filtration Units, Millipore Corp., Billerica, MA) and phosphate buffered saline (PBS, pH 7.4).[37]

SDS-PAGE Confirmation of Modification Sites. The *N*-glycans of J591 were GalNAz-tagged at the terminal GlcNAc residues with UDP-GalNAz using the β-galactosyltransferase mutant Gal-T(Y289L) (as described above). The azide groups were then clicked with DIBO−DFO or left unmodified. The *N*-glycans on the Fc of the heavy chain were then retained or removed from their asparagine residue attachment points via PNGase F treatment (see below). In addition, control, unmodified J591 was also included and either treated or left untreated with PNGase F. Mark12 Unstained Standard (Life Technologies, Carlsbad, CA) was used as a molecular weight standard. For gel analysis, antibodies were applied on NuPAGE 4−12% Bis-Tris gels and run in MOPS buffer. 200 ng antibody was applied per lane. After staining with SYPRO Ruby Protein Stain, the gels were imaged with a FUJI FLA9000 scanner with an excitation of 473 nm and a 575LP filter.

PNGase F Treatment of Antibody. J591 antibody construct (1 μg) in 10 μL TBS was denatured with 0.5% SDS and 40 mM DTT by adding 17 μL H_2O and 3 μL 10× Glycoprotein Denaturation Buffer (New England Biolabs, Ipswich, MA) and incubated at 90 °C for 10 min. For PNGase F treatment, 18 μL H_2O, 6 μL 10% NP-40 and 6 μL 500 mM sodium phosphate, pH 7.5 (G7 reaction buffer from New England Biolabs) was added. Samples were split in half, and one aliquot was supplemented with 1 μL PNGase F (New England Biolabs) and incubated overnight at 37 °C. 12 μL aliquots were loaded per lane on a SDS gel for analysis (see above).

Radiolabeling of Antibody Constructs with ^{89}Zr. For each antibody construct, 0.4−0.5 mg was added to 200 μL buffer (PBS, pH 7.4). [^{89}Zr]Zr-oxalate (2000−2500 μCi) in 1.0 M oxalic acid was adjusted to pH 7.0−7.5 with 1.0 M Na_2CO_3. After the evolution of CO_2(g), the ^{89}Zr solution was added to the antibody solution, and the resultant mixture was incubated at room temperature for 1 h. After 1 h, the reaction progress was assayed using radio-TLC with an eluent of 50 mM EDTA, pH 5, and the reaction was quenched with 50 μL of the same EDTA solution. The antibody construct was purified using size-exclusion chromatography (Sephadex G-25 M, PD-10 column, GE Healthcare; dead volume = 2.5 mL, eluted with 500 μL fractions of PBS, pH 7.4) and concentrated, if necessary, with centrifugal filtration. The radiochemical purity of the crude and final radiolabeled bioconjugate was assayed by radio-TLC. In the ITLC experiments, the antibody construct remains at the baseline, while $^{89}Zr^{4+}$ ions and [^{89}Zr]-EDTA elute with the solvent front.

Immunoreactivity Measurements. The immunoreactivity of the ^{89}Zr-DFO−DIBO/GalNAz-J591and ^{89}Zr-DFO-NCS-J591 bioconjugates was determined using specific radioactive cellular-binding assays following procedures derived from Lindmo et al.[38,39] To this end, LNCaP cells were suspended in microcentrifuge tubes at concentrations of 5.0, 4.0, 3.0, 2.5, 2.0, 1.5, and 1.0 × 10^6 cells/mL in 500 μL PBS (pH 7.4). Aliquots of either ^{89}Zr-DFO-DIBO/GalNAz-J591 or ^{89}Zr-DFO-NCS-J591 (50 μL of a stock solution of 10 μCi in 10 mL of 1% bovine serum albumin in PBS pH 7.4) were added to each tube (n = 4; final volume: 550 μL), and the samples were incubated on a mixer for 60 min at room temperature. The treated cells were then pelleted via centrifugation (3000 rpm for 5 min), resuspended, and washed twice with cold PBS before removing the supernatant and counting the activity associated with the cell pellet. The activity data were background-corrected and compared with the total number of counts in appropriate control samples. Immunoreactive fractions were determined by linear regression analysis of a plot of (total/bound) activity against (1/[normalized cell concentration]). No weighting was applied to the data, and the data were obtained in triplicate.

Stability Measurements. The stability of the ^{89}Zr-DFO-DIBO/GalNAz-J591 and ^{89}Zr-DFO-NCS-J591 bioconjugates with respect to radiochemical purity and loss of radioactivity from the antibody was investigated *in vitro* by incubation of the

antibodies in human serum for 7 d at 37 °C. The radiochemical purity of the antibodies was determined via radio-TLC with an eluent of 50 mM EDTA pH 5.0. All experiments were performed in triplicate. Both final constructs, ^{89}Zr-DFO-DIBO/GalNAz-J591 and ^{89}Zr-DFO-NCS-J591, demonstrated >96% stability at 120 h.

Chelate Number. The number of accessible DFO chelates conjugated to each antibody was measured by radiometric isotopic dilution assays following methods similar to those described by Anderson et al. and Holland et al.[40,41]

PET Imaging. PET imaging experiments were conducted on a microPET Focus rodent scanner (Concorde Microsystems). Mice bearing subcutaneous LNCaP (right shoulder) xenografts (100−150 mm^3) were administered ^{89}Zr-DFO-DIBO/GalNAz-J591 or ^{89}Zr-DFO-NCS-J591 (10.2−12.0 MBq [275−325 μCi] in 200 μL 0.9% sterile saline) via intravenous tail vein injection (t = 0). Approximately 5 min prior to the PET images, mice were anesthetized by inhalation of 2% isoflurane (Baxter Healthcare, Deerfield, IL)/oxygen gas mixture and placed on the scanner bed; anesthesia was maintained using 1% isoflurane/gas mixture. PET data for each mouse were recorded via static scans at time points between 24 and 120 h. A minimum of 20 million coincident events were recorded for each scan, which lasted between 10 and 45 min. An energy window of 350−700 keV and a coincidence timing window of 6 ns were used. Data were sorted into 2-dimensional histograms by Fourier rebinning, and transverse images were reconstructed by filtered back-projection (FBP) into a 128 × 128 × 63 (0.72 × 0.72 × 1.3 mm^3) matrix. The image data were normalized to correct for nonuniformity of response of the PET, dead-time count losses, positron branching ratio, and physical decay to the time of injection, but no attenuation, scatter, or partial-volume averaging correction was applied. The counting rates in the reconstructed images were converted to activity concentrations (percentage injected dose [%ID] per gram of tissue) by use of a system calibration factor derived from the imaging of a mouse-sized water-equivalent phantom containing ^{89}Zr. Images were analyzed using ASIPro VMTM software (Concorde Microsystems).

Acute Biodistribution. Acute *in vivo* biodistribution studies were performed in order to evaluate the uptake of both ^{89}Zr-DFO-DIBO/GalNAz-J591 and ^{89}Zr-DFO-NCS-J591 in mice bearing subcutaneous LNCaP xenografts (right shoulder, 100−150 mm^3, 4 weeks post inoculation). Tumor-bearing mice were randomized before the study and were warmed gently with a heat lamp for 5 min before administration of the appropriate ^{89}Zr-antibody construct (0.55−0.75 MBq [15−20 μCi] in 200 μL 0.9% sterile saline, 4−6 μg) via intravenous tail vein injection (t = 0). Animals (n = 4 per group) were euthanized by CO_2(g) asphyxiation at 24, 48, 72, and 96 h postinjection. In addition, to probe the ability to saturate the biomarker, an additional cohort of animals were administered ^{89}Zr-conjugates with dramatically lowered specific activity—achieved by coinjection of the standard dose of ^{89}Zr-labeled J591 mixed with 300 μg of the cold, unlabeled J591 conjugate—and euthanized at 72 h postinjection. After asphyxiation, 13 tissues (including tumor) were removed, rinsed in water, dried in air for 5 min, weighed, and counted in a gamma counter calibrated for ^{89}Zr. Counts were converted into activity using a calibration curve generated from known standards. Count data were background- and decay-corrected to the time of injection, and the %ID/g for each tissue sample was calculated by normalization to the total activity injected.

Statistical Analysis. Data were analyzed by the unpaired, two-tailed Student's *t* test. Differences at the 95% confidence level ($P < 0.05$) were considered to be statistically significant.

RESULTS AND DISCUSSION

System Design. For the study at hand, a model system was constructed using the anti-prostate selective membrane antigen (PSMA) antibody J591, the positron-emitting radioisotope ^{89}Zr, and the acyclic chelator desferrioxamine (DFO).[42,43] Over the course of the past five years, ^{89}Zr has emerged as an extremely promising radionuclide for antibody-based imaging, primarily due to the advantageous match between the relatively long physical half-life of the radiometal ($t_{1/2}$ = 3.2 days) and the multiday *in vivo* pharmacokinetic profile of many antibodies but also because of the significant stability of the chelation complex the radiometal forms with its preferred siderophore-derived chelator, DFO. Initially developed by Bander et al., J591 is a monoclonal antibody that targets an extracellular epitope of PSMA, a 100-kDa, type II transmembrane glycoprotein that is one of the best-characterized oncogenic markers for prostate cancer.[44,45] Indeed, the expression of PSMA has been shown to exhibit a positive correlation with increased tumor aggression, metastatic spread, and the development of castrate resistance or resistance to hormone-based therapies.[46] Given these critical relationships, PSMA has been a promising target for diagnostic and therapeutic agents for over a decade. Indeed, agents ranging from small molecules to antibodies (e.g., ^{111}In-7E11, which targets an *intracellular* epitope of the antigen) have been developed to target PSMA, with varying results.[47−49] J591, however, has consistently remained one of the most promising PSMA-targeted vectors, and a range of clinical trials have been reported employing J591 radiolabeled with ^{131}I, ^{177}Lu, or ^{90}Y for β-therapy, ^{225}Ac or ^{213}Bi for α-therapy, and ^{111}In for SPECT.[50−55] Ultimately, this particular collection of components was chosen for the model system not only because both the biology of J591 and the radiochemistry of ^{89}Zr are extremely well-characterized, but also because the system has tremendous clinical relevance, as non-site-selectively labeled ^{89}Zr-DFO-NCS-J591 is currently being translated to the clinic at MSKCC for patients with prostate cancer.[42,56]

Synthesis and Characterization. The first step in the investigation was the synthesis of the two basic molecular components of the system (Scheme 1). While a number of different cyclooctynes have been successfully synthesized and employed in strain-promoted click chemistry, dibenzocyclooctyne (DIBO) has been shown to strike an excellent balance between stability and reactivity and, crucially, boasts variants with convenient conjugation handles that are commercially available. Therefore, the cyclooctyne component of this system, DIBO-DFO, was synthesized via a facile isothiocyanate coupling between commercially available SCN-DFO and a DIBO variant bearing a pendant amine.[30] For the other half of the system, the activated, azide-bearing monosaccharide, UDP-GalNAz, was synthesized according to published literature procedures.[32,36] Following synthesis, both precursors were extensively chemically characterized by a variety of spectroscopic methods, including UV−vis, ^{1}H NMR, and high resolution mass spectrometry.

With these components in hand, the antibody was then site-selectively labeled with the chelator DFO in three steps

dx.doi.org/10.1021/bc400122c | Bioconjugate Chem. 2013, 24, 1057−1067

(Scheme 2). First, the antibody (1 mg) was incubated with β-1,4-galactosidase for 16 h at 37 °C in sodium phosphate buffer (pH 6.0) in order to expose the terminal GlcNAc sugar residues. Second, the antibody was incubated with UDP-GalNAz and a modified, substrate permissive β-Gal-T1 enzyme, Gal-T(Y289L), for 16 h at 30 °C in order to attach the azide-modified sugars to the heavy chain glycans. And finally, the GalNAz-modified antibody (400 μg in 1 mL TBS buffer) was incubated with DIBO-DFO (200 μL of a 2 mM solution in DMSO) for 16 h at RT in order to attach the chelator to the antibody via strain-promoted, catalyst-free click chemistry. This final step will yield two very slightly different regioisomers based on the triazole ring; however, it is extremely unlikely that such small molecular variations will have any significant effect on the *in vitro* or *in vivo* behavior of a 150 000 Da macromolecule (see Supporting Information Figure S1).

After this final step, purification via size exclusion chromatography yielded the site-selectively modified DFO-DIBO/GalNAz-J591 in 49 ± 5% yield over three steps (n = 3). For the sake of comparison, J591 was also non-site-selectively labeled with DFO via incubation of J591 with DFO-NCS (Macrocyclics, Inc.) in carbonate buffer for 1 h at 37 °C, followed by purification via size exclusion chromatography to obtain DFO-NCS-J591 in 86 ± 2% yield (n = 3). It is important to note that while the site-selective modification strategy described here is admittedly somewhat lengthy, especially compared to the nonspecific labeling methodology, the antibody is subjected to relatively mild conditions throughout the procedure.

The ubiquitous nature of heavy chain glycans on antibodies makes this methodology especially promising as a universal strategy for antibody modification, and indeed, additional experimentation confirmed that the system is both reproducible and robust. Over the course of six trials, the number of accessible chelates appended per J591 antibody construct was shown to be 2.8 ± 0.2 using a radiometric isotopic dilution assay. In parallel, a gel-based fluorescence assay was used as an alternative method to determine the number of GalNAz residues incorporated per J591 antibody. In this case, the J591 antibody was site-specifically modified with GalNAz and clicked with an AlexaFluor 488-labeled variant of DIBO (Click-iT DIBO-Alexa Fluor 488, Life Technologies, Eugene, OR). Subsequent analysis of these samples via SDS-PAGE gel electrophoresis revealed a degree of labeling (DOL) of 2.7 ± 0.2 GalNAz residues per antibody (n = 3, see Supporting Information Methods, Figure S2, and Table S1). Clearly, these two disparate but reliable assays produced statistically identical results for the number of chelators and the number of GalNAz resides per antibody, data that strongly suggests that the strain-promoted click reaction is nearly quantitative and correlates very well with previously published data demonstrating quantitative labeling using this reaction (see Supporting Information Figure S2).

To illustrate the broad applicability of this system for the labeling of a variety of different antibodies, a panel of 13 antibodies including representatives from the IgG1, IgG2, and IgG3 families of immunoglobulins were site-specifically modified with GalNAz and clicked with a DIBO compound modified with the fluorophore AlexaFluor 488 (Click-iT DIBO-Alexa Fluor 488, Life Technologies, Eugene, OR). In this case, a fluorophore-modified DIBO variant was again employed in place of its DFO-modified cousin because the gel-based method of determining degree of labeling is more reliable, more facile, and—due to the lack of ^{89}Zr—much less expensive than the isotopic dilution technique. Over the course of labeling 13 different antibodies, the degree of labeling was shown to be 3.3 ± 0.3 fluorophores/antibody, with no antibody construct bearing fewer than 2.7 fluorophores, and no conjugate containing more than 3.8 (see Supporting Information Table S1). The antibody-to-antibody reproducibility range of ±0.3 labels is unprecedented when compared to any other existing chemical antibody conjugation system that does not require genetic manipulation of the antibody.

With regard to the number of chelates per antibody, it has been well-established that IgG antibodies have, on average, two biantennary glycans, making the maximum number of possible chelates per antibody 4. However, as described above, our modification of J591 resulted in 2.8 ± 0.2 chelates/antibody, and our fluorescence labeling experiments across a variety of antibodies resulted in an average degree of labeling of 3.3 ± 0.3. There are several factors that can account for the submaximal labeling. First, our data shows that the efficiency of the chemical click reaction with DFO−DIBO is quantitative (*vide supra* and see Supporting Information Figure S2). Therefore, variation in the DOL is likely due to the primary enzymatic reactions. Along these lines, we know that a fraction of the terminal GlcNAc residues are inaccessible from the outset because we did not remove terminal sialic acids by using sialidase in conjunction with β-galactosidase. Although sialic acid content on IgGs is generally around 10% (% residue/antibody glycan), it has been shown that in some cases, sialic acid content can reach as high as 20% or more and is dependent on numerous factors including animal species, expression cell type, and cell culture conditions.[13,49,50] Typically, however, we have only seen only a 10% or less increase in the DOL when sialidase is used in conjunction with β-galactosidase (data not shown). Second, it is possible the access of the Gal-T(Y298L) enzyme to some of the terminal GlcNAc residues is restricted due to steric hindrance. Warnock et al. have shown that conversion of G0 to G1 isoforms using a wild-type GalT proceeded much more rapidly than conversion of the G1 to G2 isoforms and that subsequently the labeling efficiency of the enzyme was improved by increasing the concentration of antibody in the reaction.[57] Finally, a lack of GalNAz incorporation into the antibody glycans may result from the absence of terminal GlcNAc residues due to *N*-glycan truncation or even glycosylation site vacancy.[58] We are currently in the process of performing both CE and MS-based glycan analysis studies that will better characterize the terminal sugar configurations both before and after labeling. In any case, we demonstrate here a degree of labeling of 2.8 ± 0.2 in the case of DFO-DIBO/GalNAz-J591 and an average antibody-to-antibody DOL of 3.3 ± 0.2. If we take into account an average sialic acid content of 10%, we can reproducibly account for greater than 90% of all available terminal GlcNAc residues with a click labeling efficiency of greater than 95%.

Returning to the DFO-DIBO/GalNAz-J591 system, SDS-PAGE electrophoresis experiments were run in order to further investigate the site-selectivity of the GalNAz/DIBO-DFO conjugation methodology. In these experiments, J591 that had either been left completely unmodified, modified only with GalNAz, or modified with GalNAz and subsequently clicked with DIBO-DFO were treated with PNGaseF, an amidase that cleaves at the site between the innermost GlcNAc residue and the asparagine residues of the antibody. As shown in the resulting gel (Figure 1), the heavy chains of all three antibody

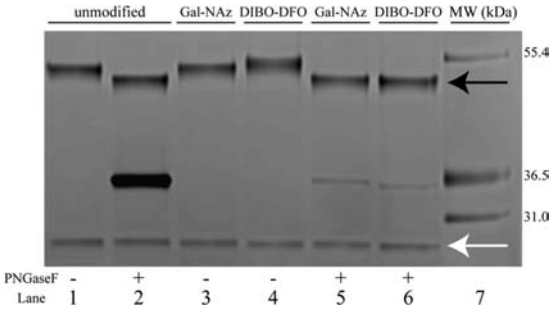

Figure 1. SDS-PAGE of unmodified (lanes 1, 2), GalNAz-modified (lanes 3, 5), or DIBO-DFO-modified (lanes 4, 6) J591 antibody constructs either untreated (lanes 1, 3, 4) or treated (lanes 2, 5, 6) with PNGaseF. The black and white arrows indicate the antibody heavy chain and light chain, respectively, and the bands at 36.5 kDa are the result of excess PNGaseF enzyme.

variants (upper bands, black arrow) were shifted to the same lower molecular weight after treatment with PNGaseF, confirming that the GalNAz and DFO modifications had been made site-selectively on the heavy chain *N*-linked glycans.

Next, both the DFO-DIBO/GalNAz-J591 and DFO-NCS-J591 antibody conjugates were radiolabeled with ^{89}Zr via incubation of the antibody (400−500 μg) with ^{89}Zr (2.0−2.5 mCi) in PBS buffer at pH 7.0−7.5 for 1 h at RT, followed by purification with size exclusion chromatography. Both antibodies were labeled in >95% radiochemical yield and purified to >99% radiochemical purity, with final specific activities of 3.5 ± 0.2 mCi/mg and 3.4 ± 0.3 mCi/mg for ^{89}Zr-DFO-DIBO/GalNAz-J591 and ^{89}Zr-DFO-NCS-J591, respectively. In further characterization, isotopic dilution experiments employing nonradioactive Zr^{4+} determined that the number of accessible chelates per antibody for each variant was 2.8 ± 0.2 for DFO-DIBO/GalNAz-J591 and 3.1 ± 0.5 for DFO-NCS-J591. Further, *in vitro* immunoreactivity experiments using the PSMA-expressing LNCaP prostate cancer cell line revealed an average immunoreactive fraction of 0.95 ± 0.02 for DFO-DIBO/GalNAz-J591 and 0.91 ± 0.02 for DFO-NCS-J591. And finally, to assay the stability of the radiolabeled bioconjugates, both ^{89}Zr-DFO-NCS-J591 and ^{89}Zr-DFO-DIBO/GalNAZ-J591 were incubated in human serum for 7 d at 37 °C. Radio-TLC with an eluent of 50 mM EDTA (pH 5.0) performed over the course of the experiment clearly illustrated that both sets of conjugates were >96% stable after the incubation period. Clearly, these data indicate that the properties of the site-selectively labeled J591 are effectively identical to those of the conventionally, non-site-selectively labeled variant. It is further of note that in this case, the site-selective modification strategy does not result in a significant improvement in immunoreactivity over its non-site-selectively labeled cousin. Indeed, this is further confirmed by the work of Holland et al., in which a non-site-specifically labeled variant of ^{89}Zr-DFO-J591 was synthesized with a slightly higher number of chelates per antibody (3.9 ± 0.3 DFO/mAb) and a slightly increased specific activity of (4.91 ± 0.03 mCi/mg) without dramatically affecting immunoreactivity (0.95 ± 0.03).[42] However, this is certainly a result of the robustness of the highly optimized antibody employed in these model systems, J591. The true benefit of site-selective conjugation and radiolabeling is far more likely to be observed with less optimized constructs, and, as a result, efforts toward the application of this labeling methodology with less robust antibodies—i.e., antibodies with which the site-selective labeling methodology will confer a more significant advantage with regard to immunoreactivity—are currently underway.

With the synthesis, characterization, and *in vitro* testing complete, the next step of the investigation was to assay the effectiveness of ^{89}Zr-DFO-DIBO/GalNAz-J591 *in vivo*. To this end, both acute biodistribution and PET imaging experiments were performed for both antibody constructs using athymic nude mice bearing subcutaneous, PSMA-expressing LNCaP prostate cancer xenografts.[42] In the biodistribution experiments, athymic nude mice bearing subcutaneous LNCaP xenografts implanted in the right shoulder were injected via tail vein with either ^{89}Zr-DFO-DIBO/GalNAz-J591 or ^{89}Zr-DFO-NCS-J591 (15−20 μCi, 4−6 μg) and euthanized at 24, 48, 72, and 96 h postinjection, followed by the collection and weighing of tissues and the assay of the amount of ^{89}Zr activity in each tissue (Tables 1 and 2, respectively). For both radioimmunoconjugates, high levels of selective uptake of the radiotracer are observed in the LNCaP xenografts, with the %ID/g increasing to maxima at 96 h of 67.6 ± 5.0 and 57.5 ± 5.3 for ^{89}Zr-DFO-

Table 1. Biodistribution Data for ^{89}Zr-DFO-DIBO/GalNAz-J591 v Time in Mice Bearing Subcutaneous LNCaP Xenografts[a]

	24 h	48 h	72 h	96 h	72 h LSA
blood	11.1 ± 4.5	7.2 ± 4.0	6.0 ± 1.6	2.9 ± 2.5	10.1 ± 1.9
tumor	14.4 ± 2.5	28.2 ± 6.8	56.3 ± 5.1	67.6 ± 5.0	28.5 ± 6.8
heart	4.6 ± 0.7	3.2 ± 1.2	3.1 ± 0.7	2.4 ± 0.8	3.2 ± 0.7
lung	5.4 ± 2.5	2.6 ± 0.3	5.4 ± 0.6	1.4 ± 0.2	5.4 ± 1.0
liver	10.3 ± 6.6	6.2 ± 4.6	5.1 ± 1.6	3.1 ± 0.9	4.7 ± 0.9
spleen	11.1 ± 3.0	7.0 ± 5.7	2.7 ± 0.9	2.0 ± 0.7	3.3 ± 1.1
stomach	0.8 ± 0.2	0.8 ± 0.1	0.5 ± 0.3	0.7 ± 0.5	0.7 ± 0.2
large intestine	1.0 ± 0.4	1.2 ± 1.2	0.4 ± 0.1	0.5 ± 0.4	0.5 ± 0.1
small intestine	2.4 ± 1.0	1.7 ± 1.3	0.9 ± 0.2	1.3 ± 1.0	1.4 ± 0.6
kidney	5.0 ± 3.5	2.4 ± 1.2	2.6 ± 1.3	2.5 ± 1.2	3.9 ± 1.4
muscle	1.6 ± 0.5	2.3 ± 0.8	2.0 ± 1.0	1.0 ± 0.4	1 ± 0.1
bone	11.1 ± 6.6	10.3 ± 2.1	8.7 ± 0.8	7.4 ± 0.9	3.4 ± 1.4
skin	3.1 ± 2.9	3.4 ± 1.6	3.1 ± 0.7	2.3 ± 0.5	5.0 ± 0.8

[a]n = 4 for each time point. Mice were administered ^{89}Zr-DFO-DIBO/GalNAz-J591 (0.55−0.75 MBq [15-20 μCi] in 200 μL 0.9% sterile saline) via tail vein injection (t = 0). For the 72 h time point, an additional cohort of animals was given ^{89}Zr-DFO-DIBO/GalNAz-J591 with dramatically lowered specific activity (LSA), achieved by the coinjection of the standard dose of the ^{89}Zr-labeled construct mixed with 300 μg of cold, unlabeled DFO-DIBO/GalNAz-J591.

dx.doi.org/10.1021/bc400122c | *Bioconjugate Chem.* 2013, 24, 1057−1067

Table 2. Biodistribution Data for ^{89}Zr-DFO-NCS-J591 v Time in Mice Bearing Subcutaneous LNCaP Xenografts[a]

	24 h	48 h	72 h	96 h	72 h LSA
blood	9.1 ± 5.3	7.4 ± 5.5	4.3 ± 4.9	7.9 ± 1.9	8.9 ± 0.5
tumor	20.9 ± 5.6	30.7 ± 6.6	48.1 ± 9.3	57.5 ± 5.3	23.5 ± 11.1
heart	4.7 ± 2.3	4.5 ± 1.7	2.6 ± 1.0	3.9 ± 1.1	2.7 ± 0.2
lung	2.3 ± 0.8	3.4 ± 2.9	2.1 ± 1.3	6.3 ± 0.9	3.7 ± 1.9
liver	6.1 ± 2.7	4.0 ± 1.3	3.8 ± 1.6	3.2 ± 0.5	5.6 ± 3.0
spleen	5.7 ± 1.9	7.5 ± 5.6	3.9 ± 1.4	4.2 ± 0.5	2.0 ± 0.3
stomach	1.9 ± 0.3	1.2 ± 0.9	0.5 ± 0.3	0.8 ± 0.2	0.3 ± 0.1
large intestine	1.3 ± 0.2	0.8 ± 0.4	0.6 ± 0.4	0.9 ± 0.3	0.5 ± 0.2
small intestine	2.4 ± 2.0	2.7 ± 1.2	0.9 ± 0.1	1.3 ± 0.2	1.1 ± 0.4
kidney	6.2 ± 0.9	4.9 ± 2.0	2.1 ± 1.1	3.3 ± 0.3	3.0 ± 0.9
muscle	0.6 ± 0.2	1.7 ± 1.8	0.7 ± 0.3	3.2 ± 1.0	0.7 ± 0.3
bone	5.4 ± 6.3	10.6 ± 3.5	9.3 ± 2.4	11.1 ± 5.6	2.6 ± 1.7
skin	0.9 ± 0.3	6.9 ± 5.7	3.1 ± 1.6	7.0 ± 1.9	7.3 ± 2.1

[a]n = 4 for each time point. Mice were administered ^{89}Zr-DFO-NCS-J591 (0.55−0.75 MBq [15-20 μCi] in 200 μL 0.9% sterile saline) via tail vein injection (t = 0). For the 72 h time point, an additional cohort of animals was given ^{89}Zr-DFO-NCS-J591 with dramatically lowered specific activity (LSA), achieved by the coinjection of the standard dose of the ^{89}Zr-labeled construct mixed with 300 μg of cold, unlabeled DFO-NCS-J591.

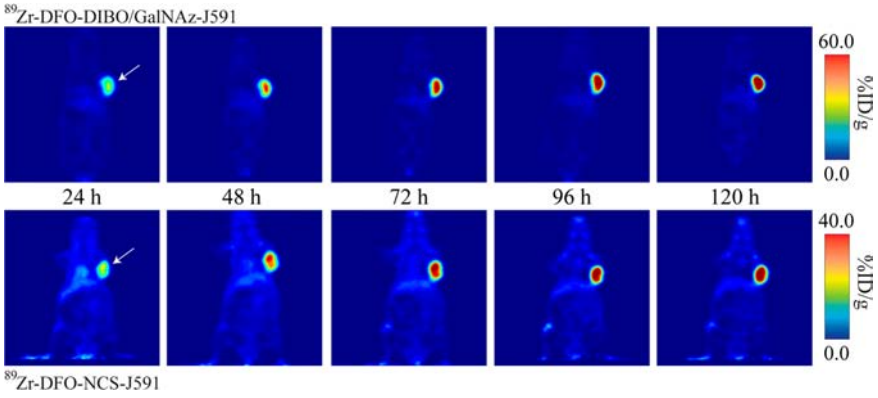

Figure 2. Coronal PET images of ^{89}Zr-DFO-DIBO/GalNAz-J591 and ^{89}Zr-DFO-NCS-J591 (11.1−12.9 MBq [300−345 μCi] injected via tail vein in 200 μL 0.9% sterile saline) in athymic nude mice bearing subcutaneous, PSMA-expressing LNCaP prostate cancer xenografts (white arrows) between 24 and 120 h postinjection.

DIBO/GalNAz-J591 and ^{89}Zr-DFO-NCS-J591, respectively. In terms of tumor-to-muscle activity ratios, ^{89}Zr-DFO-DIBO/GalNAz-J591 yielded ratios of 12.2 ± 5.1, 28.6 ± 14.3, and 68.2 ± 26.9 at 48, 72, and 96 h, respectively, while ^{89}Zr-DFO-NCS-J591 produced comparable values of 17.2 ± 9.2, 64.4 ± 27.0, and 38.1 ± 6.2 at the same three time points (see Supporting Information Tables S2 and S3).

In terms of background uptake, the two variants behaved very similarly. As is typical of antibody-based imaging agents, a decrease in the %ID/g in the blood occurred over the course of the experiment: to illustrate, with ^{89}Zr-DFO-DIBO/GalNAz-J591, the amount of activity in the blood dropped from 11.1 ± 4.5%ID/g at 24 h to 6.0 ± 1.6%ID/g at 72 h to 2.9 ± 2.5%ID/g at 96 h. The organs with the highest background uptake in both cases were the liver, spleen, and—not surprisingly given the osteophilic nature of the $^{89}Zr^{4+}$ cation—bone. For example, with ^{89}Zr-DFO-DIBO/GalNAz-J591, at 24 h, the amount of tracer uptake in the liver was 10.3 ± 6.6%ID/g, the spleen 11.1 ± 3.0%ID/g, and the bone 11.1 ± 6.6%ID/g. However, by 96 h, the tumor to tissue activity ratios for each of these tissues were 21.8 ± 6.6, 33.6 ± 12.3, and 9.2 ± 1.3, respectively, with nearly identical results for ^{89}Zr-DFO-NCS-J591. Experiments performed using ^{89}Zr-labeled constructs with drastically reduced specific activities (created by coinjecting a 300-fold excess of the unlabeled J591 constructs) resulted in dramatically decreased tumor uptake values at 72 h postinjection, specifically a reduction from 56.3 ± 5.1 to 28.5 ± 6.8%ID/g for ^{89}Zr-DFO-DIBO/GalNAz-J591 and from 48.1 ± 9.3 to 23.5 ± 11.1%ID/g for ^{89}Zr-DFO-NCS-J591, indicating antigen-selective *in vivo* targeting in both cases. Importantly, these biodistribution data were also consistent with those obtained in the original report of non-site-specifically labeled J591 by Holland et al.[42]

These biodistribution data were strongly reinforced by small animal PET imaging. In these experiments, nude mice bearing subcutaneous LNCaP xenografts were injected via tail vein with either ^{89}Zr-DFO-NCS-J591 or ^{89}Zr-DFO-DIBO/GalNAz-J591 (300−350 μCi, 100−150 μg) and imaged with static scans at 24, 48, 72, 96, and 120 h postinjection. The results (Figure 2) clearly indicate that the ^{89}Zr-DFO-DIBO/GalNAz-J591 and ^{89}Zr-DFO-NCS-J591 constructs are taken up significantly and selectively in the antigen-expressing LNCaP tumors. High blood pool activity and moderate background uptake in the heart, liver, and spleen are evident at early time points, but over the course of the experiment, this background activity is reduced and countered by a concomitant increase in signal in the tumor to a point at which it is by far the most prominent feature in the image.

Plainly, these data illustrate that this site-selective conjugation methodology creates a final radioimmunoconjugate

that is nearly identical in its *in vivo* behavior to its non-site-selectively labeled cousin. Indeed, the small animal PET imaging results are actually qualitatively suggestive of an *increase* in absolute tumor uptake and tumor-to-background contrast for ^{89}Zr-DFO-DIBO/GalNAz-J591 compared to ^{89}Zr-DFO-NCS-J591 (see scale bars in Figure 2). However, the acute biodistribution data suggests that these differences are on the cusp of statistical significance, and thus further experimentation is required to elucidate their true statistical significance and, if they are in fact significant, determine the root cause.

CONCLUSION

In summary, we have developed a methodology for the site-selective radiolabeling of antibodies on the heavy chain *N*-linked glycans that is predicated on both enzyme-mediated reactions and strain-promoted catalyst-free click chemistry. To the best of the authors' knowledge, this is one of a very few reports of an antibody modification methodology to target the heavy chain glycans as a site for selective radiolabeling and the only such strategy to avoid harsh sugar oxidation steps.[7,59] In the proof-of-concept system described here, the methodology was shown to be highly robust and reproducible and produced a ^{89}Zr-labeled radioimmunoconjugate that is identical in terms of *in vitro* and *in vivo* to an analogous, non-site-selectively labeled construct. It is important to note that while this site-selective strategy did not result in large improvements in immunoreactivity or *in vivo* behavior in this case, we ascribe this to the well-developed and optimized nature of the antibody in our proof-of-concept system, J591. We are confident that this site-selective methodology will dramatically improve the *in vitro* and *in vivo* behavior of other, less robust antibody constructs by precluding the possibility of accidental conjugation at the antigen-binding site. In addition, this methodology may also prove useful with antibody fragments retaining *N*-linked glycosylation sites, whether natural or engineered. Although the reported workflow involves three 16 h incubations, during the preparation of this manuscript we have been able to shorten the labeling process to two 16 h incubations by instituting a one-pot deglycosylation/glycosylation step. Additionally, we have improved antibody yields by replacing the gel filtration steps with low protein-binding, single-use, centrifugal concentrators. Investigations applying this new methodology to various other antibodies and labels are currently underway and are proving successful at early stages. Ultimately, we believe that this strategy could play a critical role in the development of novel well-defined and highly selective radioimmunoconjugates for both the laboratory and the clinic.

ASSOCIATED CONTENT

Supporting Information

Additional methods, diagram of the regioisomers created by the copper-free click ligation, comprehensive DIBO-AF488 labeling efficiency data, and tables of tumor-to-tissue activity concentration ratios. This material is available free of charge via the Internet at http://pubs.acs.org.

AUTHOR INFORMATION

Corresponding Author

*Phone: 1-646-888-3039. Fax: 1-646-888-3059. E-mail: lewisj2@mskcc.org.

Notes

The authors declare no competing financial interest.

ACKNOWLEDGMENTS

The authors thank Ms. Valerie Longo for aid with animal imaging experiments and Nicholas Ramos for aid in the purification of ^{89}Zr. Services provided by the MSKCC Small-Animal Imaging Core Facility and the Radiochemistry and Molecular Imaging Probe core were supported in part by NIH grant P30 CA08748. The authors also thank Drs. Pradman Qasba and Boopathy Ramakrishnan for their continued expert scientific input and support relating to the Gal-T(Y289L) enzyme expression, purification, and applications. The authors also thank the NIH (Award 1F32CA1440138-01, BMZ), the DOE (Award DE-SC0002184, JSL), the Mr. William H. Goodwin and Mrs. Alice Goodwin and the Commonwealth Foundation for Cancer Research, and the Experimental Therapeutics Center of Memorial Sloan-Kettering Cancer Center for their generous funding.

ABBREVIATIONS

PSMA, prostate specific membrane antigen; DIBO, dibenzocyclooctyne; UDP, uridine-5′-diphosphate; GalNAz, *N*-azidoacetylgalactosamine; DFO, desferrioxamine

REFERENCES

(1) Wu, A. M. (2009) Antibodies and antimatter: The resurgence of immuno-PET. *J. Nucl. Med. 50*, 2−5.

(2) Zalutsky, M. R., and Lewis, J. S. (2003) Radiolabeled antibodies for tumor imaging and therapy. *Handb. Radiopharm.*, 685−714.

(3) Zeglis, B. M., and Lewis, J. S. (2011) A practical guide to the construction of radiometallated bioconjugates for positron emission tomography. *Dalton Trans. 40*, 6168−6195.

(4) Cheng, Z., De Jesus, O. P., Namavari, M., De, A., Levi, J., Webster, J. M., Zhang, R., Lee, B., Syud, F. A., and Gambhir, S. S. (2008) Small-animal PET imaging of human epidermal growth factor receptor type 2 expression with site-specific 18F-labeled protein scaffold molecules. *J. Nucl. Med. 49*, 804−813.

(5) Gill, H. S., Tinianow, J. N., Ogasawara, A., Flores, J. E., Vanderbilt, A. N., Raab, H., Scheer, J. M., Vandlen, R., Williams, S. P., and Mark, J. (2009) A modular platform for the rapid site-specific radioalbeling of proteins with 18F exemplified by quantitative positron emission tomography of human epidermal growth factor receptor 2. *J. Med. Chem. 52*, 5816−5825.

(6) Hussain, A. F., Kampmeier, F., von Felbert, V., Merk, H. F., Tur, M. K., and Barth, S. (2011) SNAP-Tag technology mediates site-specific conjugation of antibody fragments with a photosensitizer and improves target specific phototoxicity in tumor cells. *Bioconjugate Chem. 22*, 2487−2495.

(7) Jeong, J. M., Lee, J., Paik, C. H., Kim, D. K., Lee, D. S., Chung, J. K., and Lee, M. C. (2004) Site-specific 99mTc-labeling of antibody using dihydraziniophthalazine (DHZ) conjugation to Fc region of heavy chain. *Arch. Pharm. Res. 27*, 961−967.

(8) Kampmeier, F., Ribbert, M., Nachreiner, T., Dembski, S., Beaufils, F., Brecht, A., and Barth, S. (2009) Site-specific, covalent labeling of recombinant antibody fragments via fusion to an engineered version of 6-O-alkylguanine DNA alkyltransferase. *Bioconjugate Chem. 20*, 1010−1015.

(9) Li, L., Crow, D., Turatti, F., Bading, J. R., Anderson, A. L., Poku, E., Yazaki, P., Carmichael, J., Leong, D., Wheatcroft, M. P., Raubitschek, A. A., Hudson, P. J., Colcher, D., and Shivley, J. E. (2011) Site-specific conjugation of monodispersed DOTA-PEGn to a thiolated diabody reveals the effect of incrasing PEG size on kidney clearance and tumor uptake with improved 64-copper PET imaging. *Bioconjugate Chem. 22*, 709−716.

(10) Tinianow, J. N., Gill, H. S., Ogasawara, A., Flores, J. E., Vanderbilt, A. N., Luis, E., Vandlen, R., Darwish, M., Junutula, J. R., Williams, S. P., and Marik, J. (2010) Site-specifically Zr-89-labeled monoclonal antibodies for ImmunoPET. *Nucl. Med. Biol. 37*, 289−297.
(11) Raju, T. S., Briggs, J. B., Borge, S. M., and Jones, A. J. (2000) Species-specific variation in glycosylation of IgG: evidence for the species-specific sialylation and branch-specific galactosylation and importance for engineering recombinant glycoprotein therapeutics. *Glycobiology 10*, 477−486.
(12) Wolfe, C. A., and Hage, D. S. (1995) Studies on the rate and control of antibody oxidation by periodate. *Anal. Biochem. 231*, 123−130.
(13) Clamp, J. R., and Hough, L. (1966) Some observations on the periodate oxidation of amino compounds. *Biochem. J. 101*, 120−126.
(14) Ramakrishnan, B., and Qasba, P. K. (2002) Structure-based design of beta 1,4-galactosyltransferase I (beta 4Gal-T1) with equally efficient N-acetylgalactosaminyltransferase activity: point mutation broadens beta 4Gal-T1 donor specificity. *J. Biol. Chem. 7*, 20833−20839.
(15) Clark, P. M., Dweck, J. F., Mason, D. E., Hart, C. R., Buck, S. B., Peters, E. C., Agnew, B. J., and Hsieh-Wilson, L. C. (2008) Direct in-gel fluorescence detection and cellular imaging of O-GlcNAc-modified proteins. *J. Am. Chem. Soc. 130*, 11576−11577.
(16) Boeggeman, E., Ramakrishnan, B., Kilgore, C., Khidekel, N., Hsieh-Wilson, L. C., Simpson, J. T., and Qasba, P. K. (2007) Direct identification of nonreducing GlcNAc residues on N-Glycans of glycoproteins using a novel chemoenzymatic method. *Bioconjugate Chem. 18*, 806−814.
(17) Boeggeman, E., Ramakrishnan, B., Pasek, M., Manzoni, M., Puri, A., Loomis, K. H., Waybright, T. J., and Qasba, P. K. (2009) Site specific conjugation of fluoroprobes to the remodeled Fc N-Glycans of monoclonal antibodies using mutant glycosyltransferases: Application for cell surface antigen detection. *Bioconjugate Chem. 20*, 1228−1236.
(18) Khidekel, N., Arndt, S., Lamarre-Vincent, N., Lippert, A., Poulin-Kerstien, K. G., Ramakrishnan, B., Qasba, P. K., and Hsieh-Wilson, L. C. (2003) A chemoenzymatic approach toward the rapid and sensitive detection of O-GlcNAc posttranslational modifications. *J. Am. Chem. Soc. 125*, 16162−16163.
(19) Ramakrishnan, B., Boeggeman, E., Manzoni, M., Zhu, Z., Loomis, K., Puri, A., Dimitrov, D. S., and Qasba, P. K. (2009) Multiple site-specific in vitro labeling of a single-chain antibody. *Bioconjugate Chem. 20*, 1383−1389.
(20) Agard, N. J., and Bertozzi, C. R. (2009) Chemical approaches to perturb, profile, and perceive glycans. *Acc. Chem. Res. 42*, 788−797.
(21) Khidekel, N., Ficarro, S. B., Clark, P. M., Bryan, M. C., Swaney, D. L., Rexach, J. E., Sun, Y. E., Coon, J. J., Peters, E. C., and Hsieh-Wilson, L. C. (2007) Probing the dynamics of O-GlcNAc glycosylation in the brain using quantitative proteomics. *Nat. Chem. Biol. 3*, 339−348.
(22) Tai, H. C., Khidekel, N., Ficarro, S. B., Peters, E. C., and Hsieh-Wilson, L. C. (2004) Parallel identification of O-GlcNAc-modified proteins from cell lysates. *J. Am. Chem. Soc. 126*, 10500−10501.
(23) Qasba, P. K., Boeggeman, E., and Ramakrishnan, B. (2008) Site-specific linking of biomolecules via glycan residues using glycosyltransferases. *Biotechnol. Prog. 24*, 520−526.
(24) Ramakrishnan, B., Boeggeman, E., and Qasba, P. K. (2007) Novel method for in vitro O-glycosylation of proteins: Application for bioconjugation. *Bioconjugate Chem. 18*, 1912−1918.
(25) Ramakrishnan, B., Boeggeman, E., Manzoni, M., Zhu, Z., Loomis, K., Puri, A., Dimitrov, D. S., and Qasba, P. K. (2009) Multiple site-specific in vitro labeling of single-chain antibody. *Bioconjugate Chem. 20*, 1383−1389.
(26) Vocadlo, D., Hang, H., Kim, E., Hanover, J., and Bertozzi, C. R. (2003) A chemical approach for identifying O-GlcNAc-modified proteins in cells. *Proc. Nat. Acad. Sci. U. S. A. 100*, 9116−9121.
(27) Kolb, H. C., Finn, M. G., and Sharpless, K. B. (2001) Click chemistry: diverse chemical function from a few good reactions. *Angew. Chem., Int. Ed. 40*, 2004−2021.
(28) Wadas, T. J., Wong, E. H., Weisman, G. R., and Anderson, C. J. (2010) Coordinating radiometals of copper, gallium, indium, yttrium, and zirconium for PET and SPECT imaging of disease. *Chem. Rev. 110*, 2858−2902.
(29) Sletten, E. M., and Bertozzi, C. R. (2009) Bioorthogonal chemistry: fishing for selectivity in a sea of functionality. *Angew. Chem., Int. Ed. 48*, 6973−6998.
(30) Ning, X., Guo, J., Wolfert, M. A., and Boons, G. J. (2008) Visualizing metabolically labeled glycoconjugates of living cells by copper-free and fast huisgen cycloadditions. *Angew. Chem., Int. Ed. 47*, 2253−2255.
(31) Laughlin, S. T., Baskin, J. M., Amacher, S. L., and Bertozzi, C. R. (2008) In vivo imaging of membrane-associated glycans in developing zebrafish. *Science 320*, 664−667.
(32) Laughlin, S. T., and Bertozzi, C. R. (2007) Metabolic labeling of glycans with azido sugars and subsequent glycan-profiling and visualization via Staudinger ligation. *Nat. Protoc. 2*, 2930−2944.
(33) Zaro, B. W., Yang, Y. Y., Hang, H. C., and Pratt, M. R. (2011) Chemical reporters for fluorescent detection and identification of O-GlcNAc-modified proteins reveal glycosylation of the ubiquitin ligase NEDD4−1. *Proc. Nat. Acad. Sci. U. S. A. 108*, 8146−8151.
(34) Boeggeman, E., Ramakrishnan, B., and Qasba, P. K. (2003) The N-terminal stem region of bovine and human beta1,4-galactosyltransferase I increases the in vitro folding efficiency of their catalytic domain from inclusion bodies. *Protein Express. Purif. 30*, 219−229.
(35) Holland, J. P., Sheh, Y. C., and Lewis, J. S. (2009) Standardized methods for the production of high specific-activity zirconium-89. *Nucl. Med. Biol. 36*, 729−739.
(36) Hang, H. C., Yu, C., Kato, D. L., and Bertozzi, C. R. (2003) A metabolic labeling approach toward proteomic analysis of mucin-type O-linked glycosylation. *Proc. Nat. Acad. Sci. U. S. A. 100*, 14846−14851.
(37) Vosjan, M., Perk, L. R., Visser, G. W. M., Budde, M., Jurek, P., Kiefer, G. E., and van Dongen, G. (2010) Conjugation and radiolabeling of monoclonal antibodies with zirconium-89 for PET imaging using the bifunctional chelate p-isothiocyanatobenzyl-desferrioxamine. *Nat. Protoc. 5*, 739−743.
(38) Lindmo, T., Boven, E., Cuttitta, F., Fedorko, J., and Bunn, P. A., Jr. (1984) Determination of the immunoreactive fraction of radiolabeled monoclonal antibodies by linear extrapolation to binding at infinite antigen excess. *J. Immunol. Methods 72*, 77−89.
(39) Lindmo, T., and Bunn, P. A., Jr. (1986) Determination of the true immunoreactive fraction of monoclonal antibodies after radiolabeling. *Methods Enzymol. 121*, 678−91.
(40) Anderson, C. J., Connett, J. M., Schwarz, S. W., Rocque, P. A., Guo, L. W., Philpott, G. W., Zinn, K. R., Meares, C. F., and Welch, M. J. (1992) Copper-64-labeled antibodies for PET imaging. *J. Nucl. Med. 33*, 1685−1691.
(41) Holland, J. P., Caldas-Lopes, E., Divilov, V., Longo, V. A., Taldone, T., Zatorska, D., Chiosis, G., and Lewis, J. S. (2010) Measuring the pharmacodynamic effects of a novel Hsp90 inhibitor on HER2/neu expression in mice using Zr-89-DFO-trastuzumab. *Plos One, 5*.
(42) Holland, J. P., Divilov, V., Bander, N. H., Smith-Jones, P. M., Larson, S. M., and Lewis, J. S. (2010) Zr-89-DFO-J591 for ImmunoPET of prostate-specific membrane antigen expression in vivo. *J. Nucl. Med. 51*, 1293−1300.
(43) Vugts, D. J., and Van Dongen, G. (2011) 89Zr-labeled compounds for PET imaging guided personalized therapy. *Drug Discovery Today 8*, e53−e61.
(44) Liu, H., Moy, P., Kim, S., Xia, Y., Rajasekaran, A., Navarro, V., Knudsen, B., and Bander, N. H. (1997) Monoclonal antibodies to the extracellular domain of prostate-specific membrane antigen also react with tumor vascular endothelium. *Cancer Res. 57*, 3629−3634.
(45) Liu, H., Rajasekaran, A. K., Moy, P., Xia, Y., Kim, S., Navarro, V., Rahmati, R., and Bander, N. H. (1998) Constitutive and antibody-induced internalization of prostate-specific membrane antigen. *Cancer Res. 58*, 4055−4060.

(46) Olson, W. C., Heston, W. D. W., and Rajasekaran, A. K. (2007) Clinical trials of cancer therapies targeting prostate-specific membrane antigen. *Rev. Recent Clin. Trials 2*, 182−90.
(47) Manyak, M. J. (2008) Indium-111 capromab pendetide in the management of recurrent prostate cancer. *Exp. Rev. Anticancer Ther. 8*, 175−181.
(48) Apolo, A. B., Pandit-Taskar, N., and Morris, M. J. (2008) Novel tracers and their development for the imaging of metastatic prostate cancer. *J. Nucl. Med. 49*, 2031−2041.
(49) Cho, S. Y., Gage, K. L., Mease, R. C., Senthamizhchelvan, S., Holt, D. P., Jeffrey-Kwanisai, A., Endres, C. J., Dannals, R. F., Sgouros, G., Lodge, M., Eisenberger, M. A., Rodriguez, R., Carducci, M. A., Rojas, C., Slusher, B. S., Kozikowski, A. P., and Pomper, M. G. Biodistribution, tumor detection, and radiation dosimetry of F-18-DCFBC, a low-molecular-weight inhibitor of prostate-specific membrane antigen, in patients with metastatic prostate cancer. *J. Nucl. Med. 53*, 1883-1891.
(50) McDevitt, M. R., Barendswaard, E., Ma, D., Lai, L., Curcio, M. J., Sgouros, G., Ballangrud, A. M., Yang, W. H., Finn, R. D., Pellegrini, V., Geerlings, M. W., Lee, M., Brechbiel, M. W., Bander, N. H., Cordon-Cardo, C., and Scheinberg, D. A. (2000) An alpha-particle emitting antibody ([Bi-213]J591) for radioimmunotherapy of prostate cancer. *Cancer Res. 60*, 6095−6100.
(51) Vallabhajosula, S., Smith-Jones, P. M., Navarro, V., Goldsmith, S. J., and Bander, N. H. (2004) Radioimmunotherapy of prostate cancer in human xenografts using monoclonal antibodies specific to prostate specific membrane antigen (PSMA): Studies in nude mice. *Prostate 58*, 145−155.
(52) Vallabhajosula, S., Kuji, I., Hamacher, K. A., Konishi, S., Kostakoglu, L., Kothari, P. A., Milowski, M. I., Nanus, D. M., Bander, N. H., and Goldsmith, S. J. (2005) Pharmacokinetics and biodistribution of In-111-Lu-177-labeled J591 antibody specific for prostate-specific membrane antigen: Prediction of Y-90-J591 radiation dosimetry based on In-111 or Lu-177? *J. Nucl. Med. 46*, 634−641.
(53) Vallabhajosula, S., Goldsmith, S. J., Kostakoglu, L., Milowsky, M. I., Nanus, D. M., and Bander, N. H. (2005) Radioimmunotherapy of prostate cancer using Y-90- and Lu-177-labeled J591 monoclonal antibodies: Effect of multiple treatments on myelotoxicity. *Clin. Cancer Res. 11*, 7195S−7200S.
(54) Pandit-Taskar, N., O'Donoghue, J. A., Morris, M. J., Wills, E. A., Schwartz, L. H., Gonen, M., Scher, H. I., Larson, S. M., and Divgi, C. R. (2008) Antibody mass escalation study in patients with castration-resistant prostate cancer using (111)In-J591: Lesion detectability and dosimetric projections for (90)Y Radioimmunotherapy. *J. Nucl. Med. 49*, 1066−1074.
(55) McDevitt, M. R., Ma, D. S., Lai, L. T., Simon, J., Borchardt, P., Frank, R. K., Wu, K., Pellegrini, V., Curcio, M. J., Miederer, M., Bander, N. H., and Scheinberg, D. A. (2001) Tumor therapy with targeted atomic nanogenerators. *Science 294*, 1537−1540.
(56) Deri, M. A., Zeglis, B. M., Francesconi, L. C., and Lewis, J. S. PET imaging with Zr-89: From radiochemistry to the clinic. *Nucl. Med. Biol. 40*, 3-14.
(57) Warnock, D., Bai, X., Autote, K., Gonzales, J., Kinealy, K., Yan, B., Qian, J., Stevenson, T., Zopf, D., and Bayer, R. J. (2005) In vitro galactosylation of human IgG at 1 kg scale using recombinant galactosyltransferase. *Biotechnol. Bioeng. 92*, 831−842.
(58) Hossler, P., Khattak, S. F., and Li, Z. J. (2009) Optimal and consistent protein glycosylation in mammalian cell culture. *Glycobiology 19*, 936−949.
(59) Alvarez, V. L., Wen, M. L., Lee, C., Lopes, D., Rodwell, J. D., and McKearn, T. J. (1986) Site-specifically modified 111In labelled antibodies give low liver backgrounds and improved radioimmunoscintigraphy. *Nucl. Med. Biol. 13*, 347−352.